EFFECTS OF ABBRASIVE PARTICLES ON PROJECTED FATIGUE LIFE OF NYLON CLIMBING ROPE

Casey Johnson, Charlie Klonowski

Advisor: Dr. Vanasupa

Objective: To characterize the effect of sediment on the fatigue strength of static rope.

Abstract:

When climbing rope is used outdoors, it is exposed to foreign particles such as sand and silt. These particles can potentially work their way through a rope's sheath and damage the load bearing core decreasing the rope's strength without exhibiting obvious wear. This project quantified the effect of abrasive particles on the fatigue life of nylon climbing rope. The experimental design involved 18 pieces of static nylon rope of kernmantle construction. 9 of these samples were agitated in a well graded slurry of water, silt, sand and soil, and left to sit for 24 hours. The remaining 9 samples were submerged in clean water for the same period. Two sections of rope from each the dirty and clean groups were exposed to the prescribed fatigue treatment. After this treatment, each rope section was tensile tested. Comparisons were made between the strengths of the dirty rope samples and the clean rope samples. It was found that exposure to abrasive particles decreases the fatigue life of the rope. It should be noted that the clean and dirty rope segments had identical strengths before fatigue treatment (5500lb break strength), the same as that of new rope (100% overall strength). Once exposed to fatigue treatment, the dirty ropes' overall strength dropped much more quickly than that of the untreated rope. After 500 fatigue cycles, the treated rope experienced a drop in strength of 79% as opposed to the untreated rope which only saw a 2% drop in strength. From this it has been determined that abrasive particles do decrease the fatigue life of nylon fiber ropes.

Table of Contents

Introduction:

Rock climbing has grown in popularity in recent years. Barber, Peacock and Bericchia (2010) suggest that over 9 million people participate in rock climbing activities every year in the US alone. As more people participate in this sport with a high risk of injury, a greater emphasis must be placed on safety. A large part of safety has to do with proper rope maintenance procedures. A lack of proper care can lead to a greater probability of injury or death.

One important aspect of safe climbing practice is proper cleaning and maintenance of equipment. This is especially important in the case of the climbing rope. Unlike other pieces of climbing equipment such as carabineers, belay devices, cams and nuts which may be constructed out of aluminum or stainless steel, ropes are made from a synthetic nylon weave which is inherently more prone to wear. As long as the condition of the rope can be accurately assessed visually, this is not a concern. Ropes that are obviously in poor condition can be retired and replaced. The danger comes when the load bearing core suffers damage without the protective sheath displaying any loss of integrity. This could potentially occur if particles made their way into the core fibers causing wear without damaging the sheath. This danger is minimized by proper rope maintenance, i.e. proper use, cleaning and storage. This is pertinent because while a lot of testing and study has been done on the other areas of rope wear (direct contact with belay devises, rocks, etc.) how rope strength is potentially decreased by improper rope care has not been sufficiently studied.

Much is known about static climbing ropes. Properties like load bearing capacity, and tensile strength, as well as the effects of heavy loading on tensile strength and how strength reduces over time have been well studied. Not much information is available concerning how exposure to abrasive particles affects tensile strength. This experiment investigates this effect by developing a basic understanding of how different soil types wear on dynamic climbing rope. The rope being studied is 11mm diameter nylon kernmantle static climbing rope, with a cylindrical braided sheath protecting the load-bearing core consisting of ten main strands. The idea is that particles could pass through the protective sheath, and rub against the core fibers over time through use, reducing the integrity of the rope. Note that a standard safety check before using a climbing rope involves conducting a visual check of the entire length of the rope. If the sheath material appeared normal, but the inside core were damaged, this safety check would fail to indicate that the rope was unfit for use.

Technical Background:

The specific type of nylon that the core is made up of is Nylon 6, a material with properties similar to nylon 6,6 but that doesn't violate its patent. Nylon 6 and nylon 6,6 have equally shared about 90% of the nylon market since their introduction into mainstream use 60 years ago. These two nylons' superiority comes from their high strength to weight ratio, high breaking elongation, excellent elastic properties and dyeability.

Composition:

The name nylon 6,6 refers to the numbers of carbons donated by the monomers. For nylon 6,6 both the diamine and the diacid each donate 6 carbons to the polymer chain. Since nylon 6 is a copolymer, each repeating unit in the nylon chain consists of a diamine and diacid monomer.

The specific chemical elements included in nylon 6 are identical to those of nylon 6,6. These elements include carbon, hydrogen, oxygen and nitrogen.

Processing:

Benzene is an organic compound with chemical formula C_6H_6. It was first discovered in the byproduct of coal tar in the 1800's but is more commonly found in petroleum and crude oil. Benzene is also found in nature as well as created industrially. Benzene, fated to become nylon 6, is reacted with hydrogen to create cyclohexane. The conversion of benzene to cyclohexane is stoichiometric and almost complete leaving typically less than 50 ppm benzene remainder.

More than 90% of the cyclohexane produced this way is used to create the precursor caprolactam for nylon 6,6 and nylon 6. The first step in synthesizing caprolactam is the oxidation of cyclohexane into a cyclohexanone-cyclohexanol mixture known as KA fluid. Cyclohexanone is then separated from the KA fluid by first dehydrating the mixture, then vacuum fractionation. The excess cyclohexanol is then dehydrogenated into cyclohexanone through a phenol route.

The pure cyclohexanone is then carried through oximation followed by Beckman rearrangement to produce caprolactam. Nylon 6 is produced using the precursor molecule Caprolactam, an organic compound with the chemical formula $(CH_2)_5C(O)NH$.

To polymerize pure caprolactam to make nylon 6, it is first heated to 533K with water in an inert atmosphere of nitrogen, held there for four to five hours, then drawn through spinnerets to form individual fibers. Nylon 6 has many applications, but some of those fibers will be cooled, and woven into strands that will create the core of a climbing rope.

When extruded into fibers through a spinneret, the individual polymer chains preferably align due to viscous flow. The fibers are often cold drawn afterwards, further aligning the chains and increasing their crystallinity. This increased crystallinity augments the tensile strength of the fibers.

Structure:

Nylon 6 and Nylon 6,6 have similar structures to each other as seen in Fig. 1.

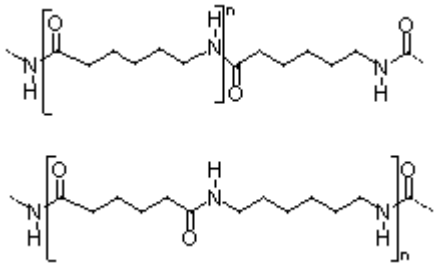

Fig. 1 Nylon 6 (above) has a polymer backbone with an oxygen double bond and a nitrogen hydrogen group. The nearly identical nylon 6,6 monomer is shown below, the only difference being the location of the middle oxygen double bond and the location where the monomer is repeated at.

The effect structure has on the properties is dichotomous between the amorphous regions and the crystalline ones. The polymer structure of nylon 6 is such that there are no large protrusions branching off of the chain which allow a high degree of elasticity in the bulk material. In other words, the amorphous structure of the nylon 6 chains grants the material its elastic properties. On the other hand, the planar amides (CO-NH) are extremely polar, preferably aligning to form hydrogen bonds between adjacent chains, and creating regions of semi-crystallinity. These regions with lamellar crystals are what give nylon 6 its strength and rigidity properties. Due to its symmetry and regularity, nylon 6 has both frequent and large regions of crystallinity, so many that it is nearly impossible to quench the molten material into a completely amorphous bulk solid.

Properties:

The resulting fibers are tough and possess a high tensile strength of between 4.0 and 7.2 grams/denier [g/d]. The fibers also have a high elastic recovery being 98% after a 3% stretch. They have excellent chemical and abrasion resistance, and have between 2.8% and 5% water absorption capacity.

The numbers outlining the properties of nylon 6 fibers are given in ranges due to their dependency on degree of crystallinity and molecular weight. These two characteristics are controlled by the polymerization, spin, draw and quenching processes as explained earlier.

The melting temperature of nylon 6 also makes it an attractive material for a great deal of applications. With a melting temperature of 220˚C (428˚F), nylon 6 can be used in a wide range of temperatures. Also, nylon 6 maintains its semi-crystallinity and high strength almost to its melting temperature.

Procedure:

The first portion of this project involved determining what effect different soil types have on rope fibers when they are rubbed into the fibers. To determine this effect, four soil samples, a coarse sand, a fine sand, a silty sand and a sandy clay, were collected from the Cal Poly Geotechnology lab with the help of Dr. Gregg Fiegel see Fig. 2. Then a length of 11mm diameter nylon kernmantle dynamic climbing rope was cut into four 5 inch sections, see Fig. 3. For each section, the core was separated from the sheath and the cut fibers melted with a butane torch to prevent unraveling, see Fig. 4. Each segment of core and sheath material was assigned to one soil type for testing.

(a) (b) (c) (d)

Fig. 2 Soil samples (a) coarse sand, (b) fine sand, (c) silty sand and (d) sandy clay

Fig. 3 Rope cut into 5 inch sections

Fig. 4 Core separated from sheath and welded

Testing was conducted by fixing the sheath material to a plywood board with flat-head tacks, then applying a small amount of soil (about 1 tablespoon) to the sheath material as well as a small amount of water. The core material was then rubbed manually against the sheath material and soil for 1 minute intervals for the first seven minutes, then for a three minute interval, then for two five minute intervals for a total of twenty minutes. Pictures of the core and sheath were taken, the sheath and core were rinsed, observations of the core fibers, and an estimation of % wear (indicating % total fibers severed)

were made at the end of each interval. Note that the clay soil was wetted beforehand to make it more malleable.

The second phase of testing was directed toward determining the effect application of soil particles have on the fatigue life of synthetic rope. To do this, 60 feet of 10mm static nylon rope of kernmantle construction, manufactured by BlueWater Ropes was purchased from Mountain Air Sports in San Luis Obispo. This 60ft section of rope was then cut into eighteen sections, each three feet long. Then half of these ropes were treated with soil particles. After analyzing the result of the first phase of testing, it was decided that a well graded mix of clay, silt, sand, and organic matter would be used to treat the rope. To achieve this, half a cubic foot of Redi-Grow Top Soil and one gallon of water were mixed in a 5gallon bucket and the ropes to be treated were placed in the mud slurry and agitated with a wooden rod for 5minutes to encourage the soil particles to migrate through the sheath fibers into the core. The ropes were then left submerged in the slurry for 24hours then removed and air-dried, without washing. The other half of the rope sections were submerged in a bucket filled with clean water and agitated for 5minutes with a clean wooden rod, left submerged for 24hours, then removed and air-dried. The ropes were treated in this fashion as opposed to being exposed to dry soil, because when ropes are used in the field, they are often exposed to non-ideal, muddy conditions, and it was thought that a mix of water and soil particles would be more likely to exhibit an effect on the fatigue life of the ropes.

The next step was to apply a fatigue treatment to the rope segments. The standard method for fatigue treatment of rope is as follows:

> *"…ropes were cycled over mild steel sheaves with low-friction bearings…The center section (approx.. 1200mm) of each rope was subjected to two bend cycles (straight, bent, straight, bent, straight) per machine cycle, the "double bend zone" or DBZ. On either side of the DBZ was a 950mm section (one-half a sheave circumference) subjected to only one bend cycle (straight-bent-straight) per machine cycle – the "single bend zone" or SBZ.*
>
> *Sheaves used in these tests had a sheave tread diameter of 570mm and a sheave groove diameter of 42mm. The test machine was cycled at a rate of 150 cycles per hour. Ropes were tested in pairs, i.e.identical ropes were loaded onto each end of the machine. The rope that failed first was taken and examined for failure mode and forensic analysis. The companion rope was taken for residual strength testing.*
>
> *Once the test was started, measurements of the rope external temperature were taken using an optical laser pyrometer. The pyrometer is much simpler to use compared with embedded thermocouples and does not interrupt the test or interfere with the test specimen. Earlier testing…has indicated very good agreement between thermocouple measurement and the pyrometer measurement. Maximum rope temperatures were consistently observed in the double-bend-zone" [6]*

Ideally, this method of fatigue testing would have been used. However, in the interest of time and due to a restricted budget, an alternate method of testing was devised. Instead of using expensive fatigue

testing equipment to wear the rope, the rope was fatigued by an operator. To do this, the operator donned a climbing harness, and attached one end of the rope segment to the harness with a prussic loop, passed the rope through an aluminum D-shaped carabineer, and attached the other end of the rope to a bucket filled with approximately 40lb of sand (the same amount of sand was used for every rope segment). This weight was decided on because a large tension force was desired to adequately fatigue the rope in a reasonable amount of time, however if any more sand was added, then the body weight of the operator was insufficient to pull the rope over the carabineer, as the opposing friction force was too great. The operator then pulled the rope down by performing a squat motion, repeating the motion for as many cycles as the test required. The actual fatiguing of the rope took place at the point where the rope passed over the carabineer.

While the recommended test method specified fatiguing the ropes to failure, this was accomplished over 7000-12000 cycles, which was unrealistic for this testing method. It was therefore decided that the ropes would be fatigued over hundreds rather than thousands of cycles, and the residual strength would be used to determine how quickly the residual strength of the rope decreased. It was then decided that two rope sections from the treated population and two from the control would be exposed to 100 cycles, four more to 200 cycles, four more to 300 cycles, four more to 400 cycles, and one segment each from the treated and control populations would be treated with 500 cycles.

This fatigue treatment was executed, and the ropes were ready for tensile testing to determine residual strength. The Materials Engineering department's Instron tensile tester at Cal Poly was used to test all the rope segments. Given the length of the rope segments, and the grips available on the machine, the rope segments were tied into loops composed of approximately 1foot of rope with double fishermen knots. This knot was chosen for its high strength and ability to resist slipping during testing. The testing machine was then loaded to approximately 2.6kN before the initial sample length was recorded and entered into the machine. This was to help pull out the slack in the rope and in the knots. The tensile test was run and stress-strain and ultimate fail strength was recorded for all segments of rope. Please note that the two samples of clean rope exposed to 100 fatigue cycles were damaged during preparation for tensile testing and are not included in the data analysis.

Results:

The raw data from the tensile test was collected and summarized in a graph with tensile strain on the x-axis and maximum load on the y-axis. Plots of data color coded for each iteration are seen in Fig. 5.

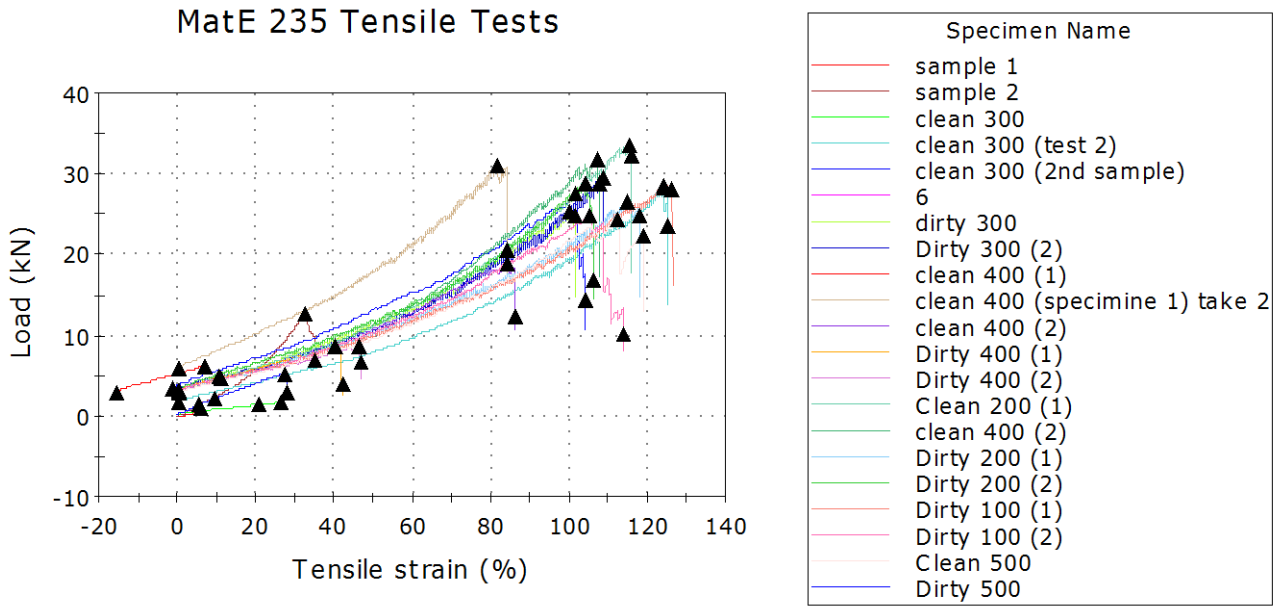

Fig. 5 This graph shows the maximum breaking strength of all the samples. The clearly visible steps after maximum load is reached is due to the core and sheath fibers breaking gradually in sections instead of all simultaneously. Some samples were used to calibrate the machine and determine testing procedure which is the reason for the low values in some tests.

More raw data shown in Table I further quantifies the breaking strength of the rope samples. Most notably from this table is the tensile strain at break as a percentage. This percentage remains relatively unaffected through the 300 cycles conditioned samples, but at 400 cycles the strain at failure begins to degrade significantly.

Table I: Raw Data from Tensile Test of 10 mm Static Rope Samples

	Specimen label	Maximum Load (N)	Tensile stress at Maximum Load (MPa)	Tensile strain at Break (Standard) (%)
1	Dirty 100-1	28601.0	364.16	126.4
2	Dirty 100-2	24831.8	316.17	114.1
3	Clean200-1	33545.2	427.11	116.0
4	Clean200-2	31708.2	403.72	107.8
5	Dirty 200-1	26513.3	337.58	118.1
6	Dirty 200-2	28700.8	365.43	106.3
1	Clean300-1	28213.0	359.22	125.4
2	Clean300-2	27495.7	350.09	104.3
3	Dirty 300-1	25270.9	321.76	101.8
4	Dirty 300-2	29488.6	375.46	108.8
5	Clean400-1	31075.9	395.67	84.4
6	Clean400-2	18742.5	238.64	86.3
7	Dirty 400-1	8579.6	109.24	42.1
8	Dirty 400-2	8738.8	111.27	46.7
15	Clean 500	24434.3	311.11	119.0
16	Dirty 500	5168.8	65.81	28.2

The raw tensile test data was then organized and grouped by cycle exposure. The tensile test data for ropes exposed to 100 cycles are shown in Fig. 6, for ropes exposed to 200 cycles in Fig. 7, for 300 cycles, Fig.8, for 400 cycles, Fig. 9 and for 500 cycles, Fig. 10.

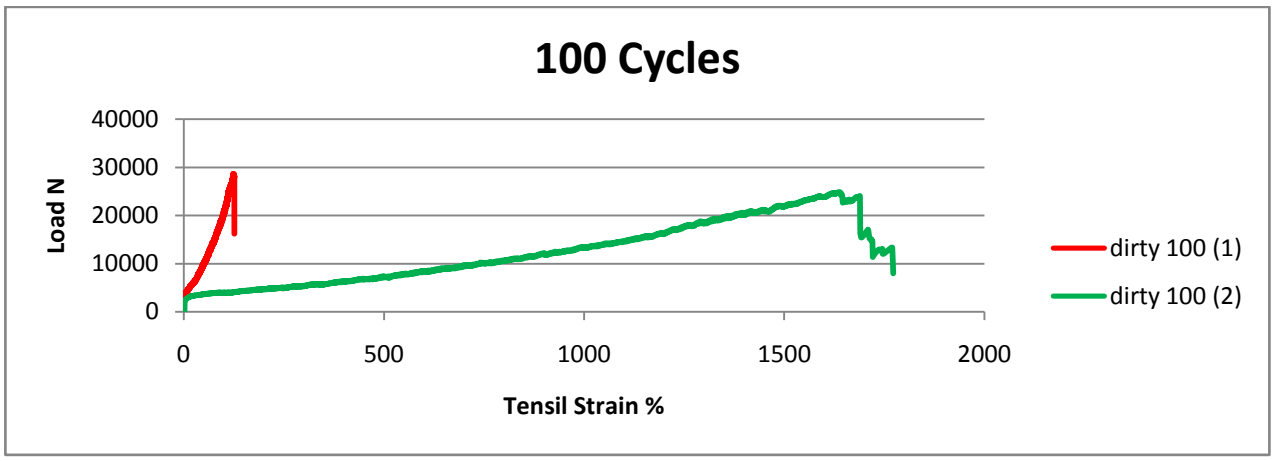

Fig. 6 Tensile test plot for ropes exposed to 100 fatigue cycles. Please note, only the treated samples of rope were tensile tested, as the untreated sections were damaged during preparation.

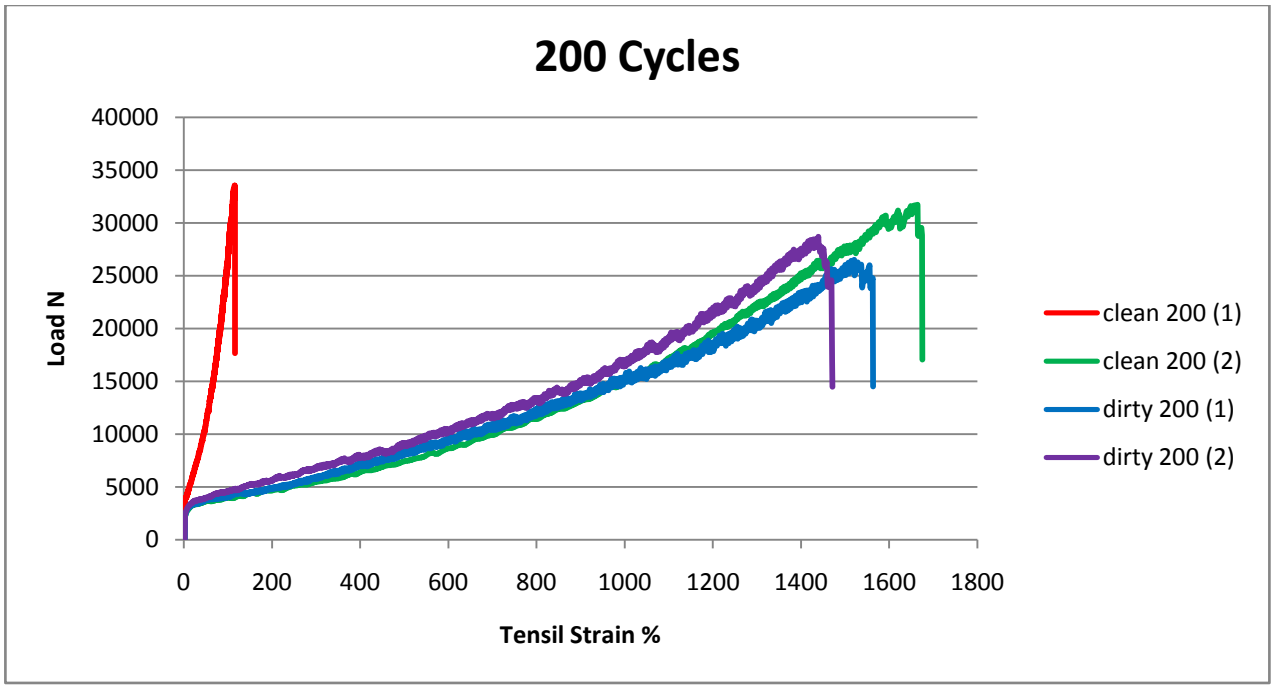

Fig. 7 Tensile test plot for ropes exposed to 200 fatigue cycles

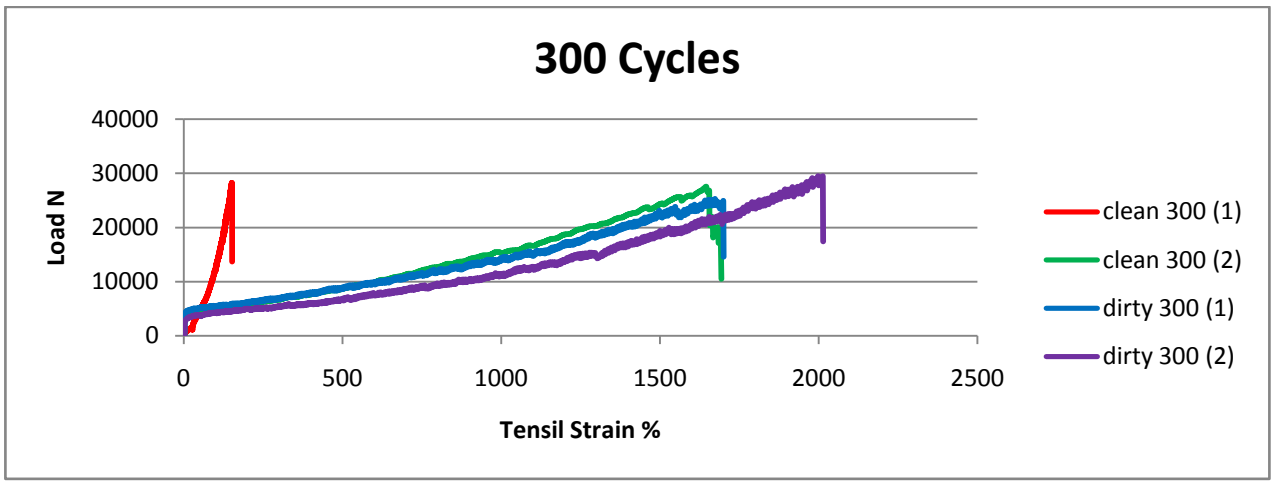

Fig. 8 Tensile test plot for ropes exposed to 300 fatigue cycles

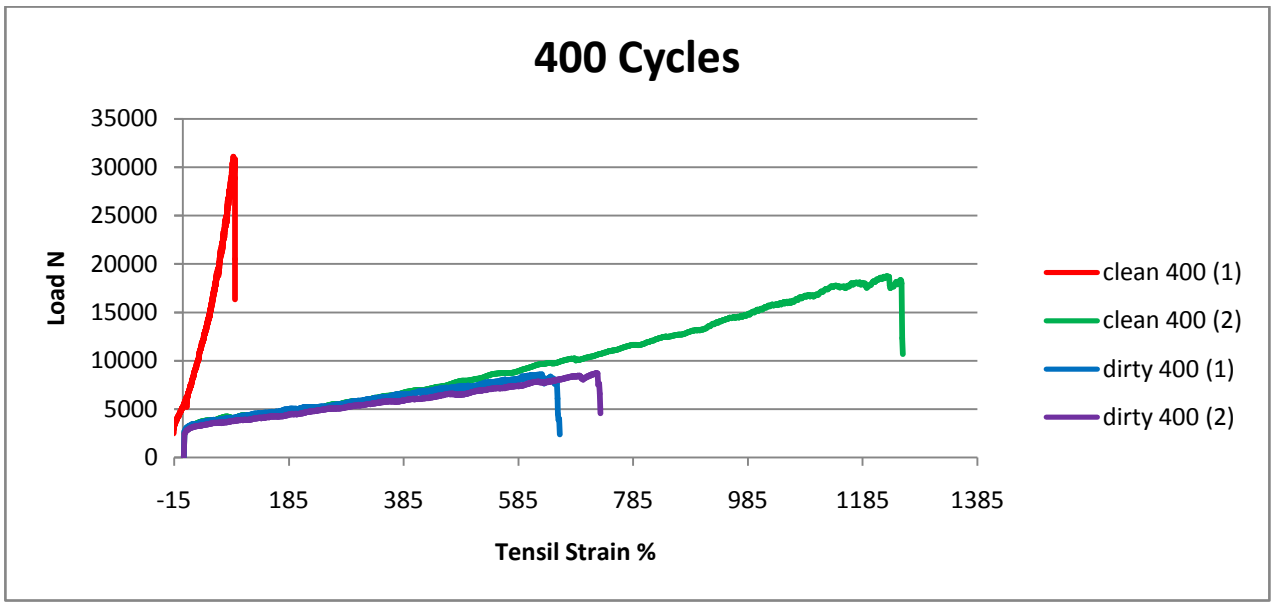

Fig. 9 Tensile test plot for ropes exposed to 400 fatigue cycles

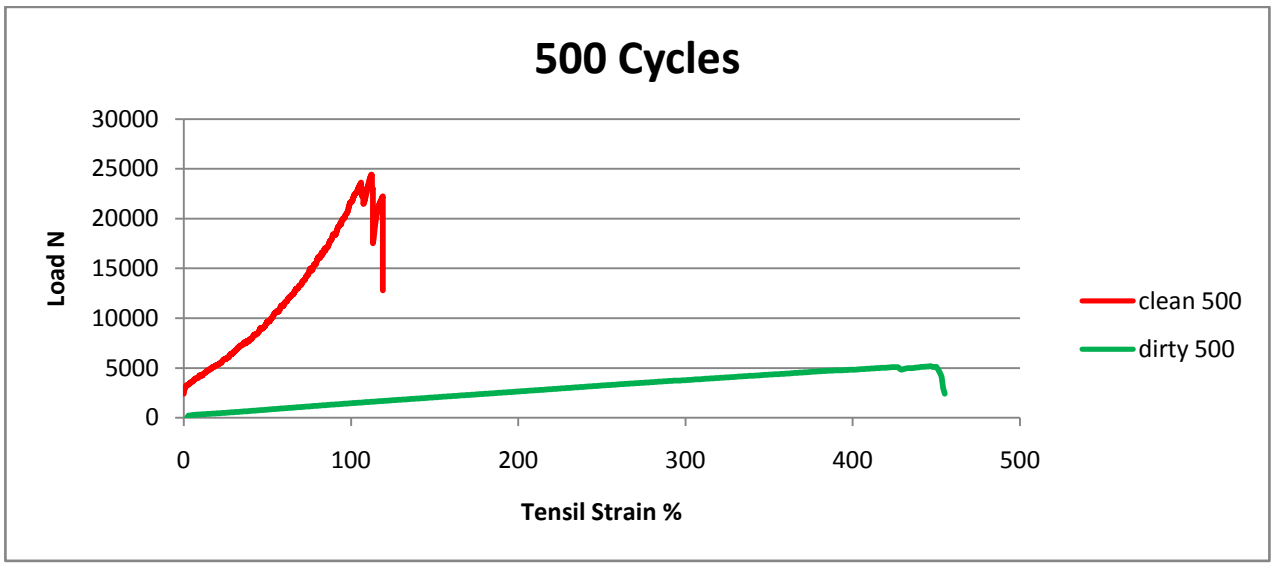

Fig. 10 Tensile test plot for ropes exposed to 500 fatigue cycles. One rope from each population was exposed to 500 cycles in the interest of time.

By simply looking at these plots, it is evident that as the rope is exposed to more fatigue cycles, the treated ropes exhibit considerably reduced residual strength.

A two sample t-test was run on the data to compare the mean breaking strength of the dirty samples with the mean breaking strength of the clean samples in order to see if there was a statistically significant drop in strength between the two. The relevant statistical data is summarized in Table II. With all the assumptions of a two sample t-test satisfactorily met, a t-value of 1.794 was obtained.

Table II: Statistical analysis of maximum load at failure data for 10 mm static rope samples

Cycles	Dirty (1)	Clean (2)	Statistic	Value
100	28601.08	26566.1	$\bar{x}_1$	20654.871
100	24831.82	24452.6	$\bar{x}_2$	27246.13
200	26513.38	33545.25	s^2_1	100826944
200	28700.8	31708.27	s^2_2	20695160
300	25270.98	28213.01	n_1	9
300	29488.6	27495.78	n_2	9
400	8579.59	31075.93	k	16
400	8738.83	18742.54	t	1.79375
500	5168.76	24434.39		

With a 95% confidence interval and 16 degrees of freedom, the t-value required to reject the null hypothesis and confirm a statistically significant difference in the means of these two groups is 1.746. With a calculated t-value of 1.794, we can be 95% confident that there is a significant drop in maximum

breaking strength between the dirty samples and the clean ones. This drop must be the result of the sediment particles ground into static ropes.

A graphical depiction of the raw data is shown in Fig. 11. In this figure the gradual drop off of break strength can be seen visually after the 300 fatigue cycles condition.

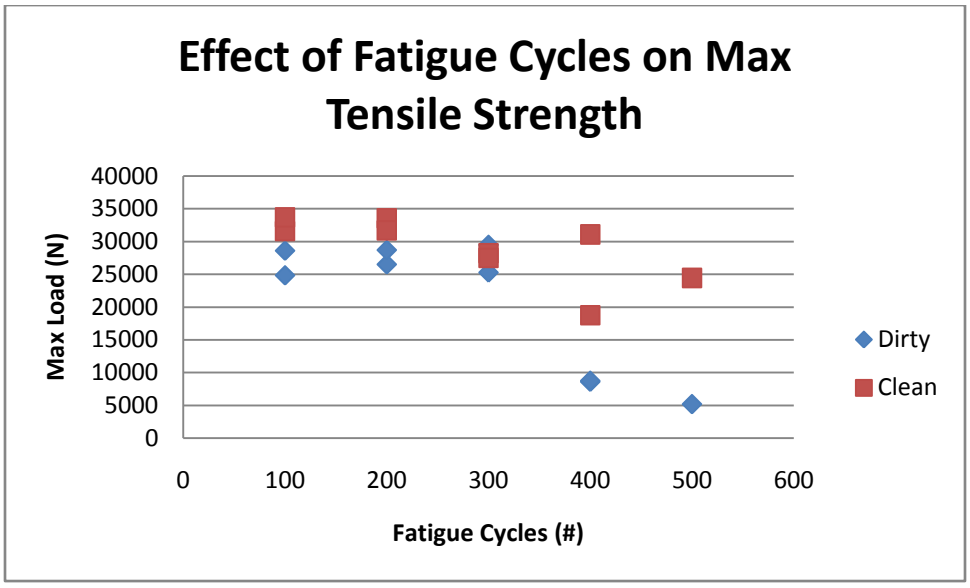

Fig. 11 As fatigue cycles increases, there is initially no significant decrease in maximum load at break. After 300 cycles the fatigue begins to significantly affect the max load at failure.

Except for one sample in the 300 cycle group, all of the dirty ropes failed at lower maximum loads than the clean ropes given the same fatigue treatment. For both the clean and dirty samples, there was a gradual drop on maximum load at failure over the 100, 200 and 300 cycle conditions. While the clean samples continued this trend, there was a significant drop off in maximum tensile strength for the dirty ropes after 400 cycles. Although a gradual trend sloping downward, there is no statistically significant drop in tensile strength for the clean rope across all the fatigue cycles conditions. There is a statistically significant difference between the clean ropes and the dirty ones at the 400 and 500 fatigue cycle conditions. This indicates that proper care of a climbing rope has a cumulative effect that is most noticeable at higher fatigue. It is confirmed that proper care involving routine cleaning can help preserve overall strength in the long run by disallowing the buildup of particles within the core of the rope.

Discussion

The data gathered from the first phase of testing indicates that soil composed of silty sand caused the most apparent damage to the core fibers after 20 minutes of rubbing, whereas the coarse sand caused the least amount of wear, see Fig. 12 , Fig. 13 and Table 1. This was contrary to expectations. It was thought that larger particles would have more of an effect on the core fibers. It seems that the coarse sand had less of an effect on the fibers because the particles themselves were somewhat rounded, offering fewer sharp edges for the fibers to be cut by. Also, during rubbing, many of the sand particles were pushed off of the sheath material, whereas the finer soils tended to adhere to the sheath material better. It may be that silty sand had the most effect because of the combination of fine particles and sand particles. The fines adhered the sand particles to the sheath material, which increased contact with the core fibers. Another possibility is that the sand particles in the silty sand were more angular than those in the fine and coarse sand samples.

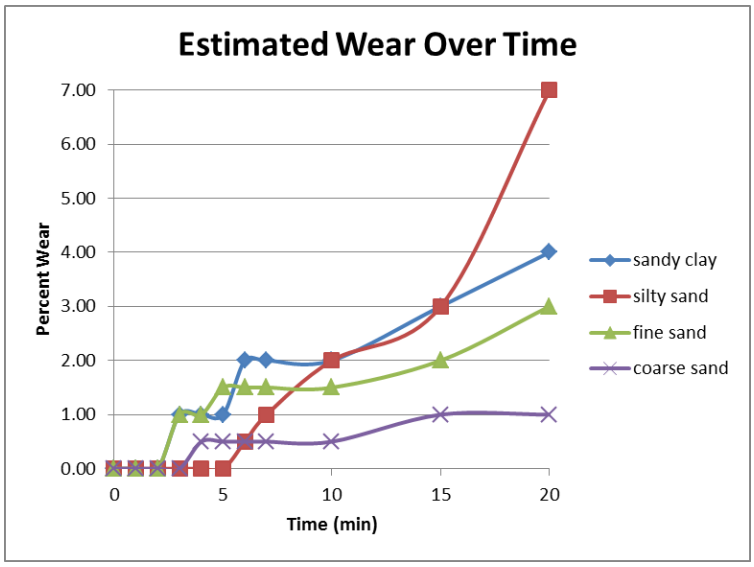

Fig. 12 Graphical representation of estimated core wear over time for each soil type

(a)

(b)

(c)

(d)

(e)

Fig. 13 Core samples (a) before treatment, and after treatment for (b) fine sand, (c) coarse sand, (d) sandy clay and (e) silty sand

Table III: Observations and wear estimations for each of the four soil samples.

Sample 1-Sandy Clay				
Time (min)	Observations	Estimated % Wear	Date	Time
0	Core appears clean with no frayed portions	0	11/24/2011	11:30am
1	core shows discoloration (particles lodged in fibers), slight fraying	0		
2	slightly more fraying	0		
3	obvious fraying (some bunching of frayed fibers)	1		
4	increased fraying seven out of 10 main strands show bunched frays	1		
5	no noticalbe difference	1		
6	slightly more fraying, some larger particles embedded in fibers	2		
7	same	2		
10	no noticalbe difference	2		
15	more fraying	3		
20	more fraying	4	11/25/2011	11:54am
Final assessment	this soil did not have as much effect as I expected. The core is damaged, but none of the main strands wore through. There is obvious damage to the core material.			
Sample 2-Silty Sand				
Time (min)	Observations	Estimated % Wear	Date	Time
0	no frays, no discoloration	0	11/25/2011	12:17pm
1	slight fraying	0		
2	slightly more fraying	0		
3	slight bunching on 1 of the main strands	0		
4	little change	0		
5	little change	0		
6	2 of main strands show notable fraying	0-1		
7	1 strand shows significant wear and fraying with signs of fraying on 4 others	1		
10	1 strand shows serious fraying 1 with significant fraying	2		
15	substantial fraying on 9 strands	3		
20	more fraying	5-10		
Final assessment	1 strand very frayed (about 1/3 worn through)			
Sample 3-Fine Sand				
Time (min)		Estimated % Wear	Date	Time
0	clean with no fraying	0	11/26/2011	1:40pm
1	slight fraying on one strand	0		
2	slight fraying and wear	0		
3	little change	1		
4	4 strands frayed	1		
5	little change. note: sand particles seem to be being pushed to side, off of sheath	1-2		
6	slightly more wear	1-2		
7	fraying and bunching	1-2		
10	little change	1-2		
15	little change	2		
20	slightly more wear	3		
Final assessment	2 strands substantially worn. No discoloration due to lack of fines may affect my visual assessment.			
Sample 3-Coarse Sand				
Time (min)		Estimated % Wear	Date	Time
0	clean no frays	0	11/26/2011	3:00pm
1	slight fraying, 1 strand	0		
2	no change	0		
3	no change. Note: Larger sand grains get pushed away from sheath material faster	0		
4	2 strands somewhat frayed	0-1		
5	no change	0-1		
6	no change	0-1		
7	slight fraying on all strands, still not much	0-1		
10	same	0-1		
15	2 strands show significant fraying	1		
20	3 strands show significant fraying	1		
Final assessment	3 strands substantially frayed, 1 strand shows almost no wear.			

During the fatiguing process of the dirty ropes, a noticeable amount of heat was produced between the ropes and the belay device. This heat was negligible up to the 300 fatigue cycle conditions, but became a factor to be considered at the 400 and 500 cycle conditions. The clean ropes do not appear to have sustained any significant heating during the fatigue treatment. However, in the treated samples, the heat caused a noticeable change of diameter and stiffness in the 400 and 500 cycle samples. This change in stiffness is reflected in the measured strain at failure during testing of these samples. The effect that this frictional heat had on the core fibers is that they were fused together into an amorphous mass and lost most of their strong fibrous quality along the major axis.

To reinforce our assertion that melting of the core fibers had an effect on the residual strength of the rope samples, a heat transfer analysis was conducted with the assistance of Dr. Kim Shollenberger, professor of Mechanical Engineering at Cal Poly. A statics analysis was first conducted to determine the force due to friction and subsequent frictional heating of the carabiner, see Apendix B. To simplify calculations, it was assumed that the rope and carabiner were mass-less, that the carabiner was fixed, that the angles of the rope were constant, that there was no heat loss due to radiation or through the rope (which is a valid assumption due to nylon's low thermal conductivity), and that there was no acceleration during the up or down stokes of the fatigue treatment, the acceleration and deceleration at the bottom and top of the strokes were ignored. An initial Lump Capacitance heat transfer analysis was then conducted to get a general idea of what temperature the carabiner would approach at steady state. This analysis indicated that the carabiner would reach a temperature of 549˚C -1074˚C depending on what value is used for the heat transfer coefficient of air. How the temperature varied over time was calculated and the results were plotted, see Fig. 14.

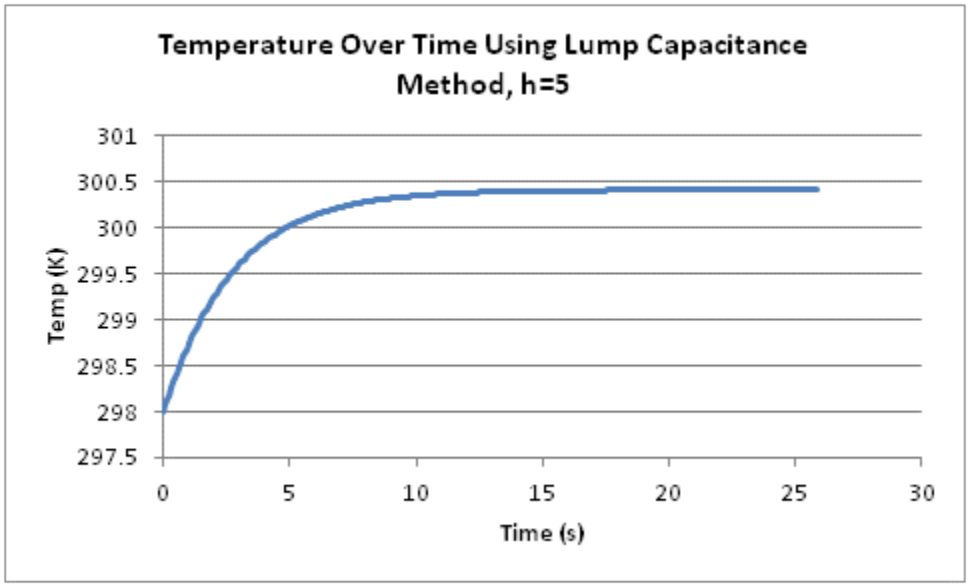

Fig. 14 Temperature over time using Lump capacitance method.

When more accurately modeled as a fin, with temperature varying with length, the steady state base temperature ranged from 1391K to 2440K, as seen in Fig. 1.

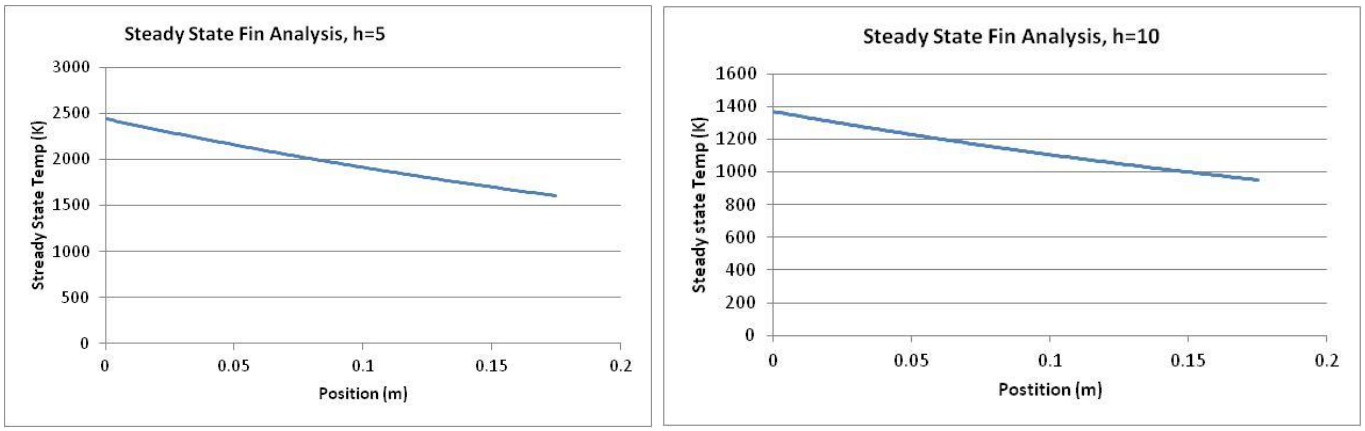

(a) (b)

Fig. 15 Steady state analysis of carabiner modeled as a pin fin with (a) h=10 and (b) h=5.

Finally, a more accurate finite difference method (FDM) analysis of the system was conducted using Excel©, modeled with 1-D heat conduction through the carabiner, see Fig. 16.

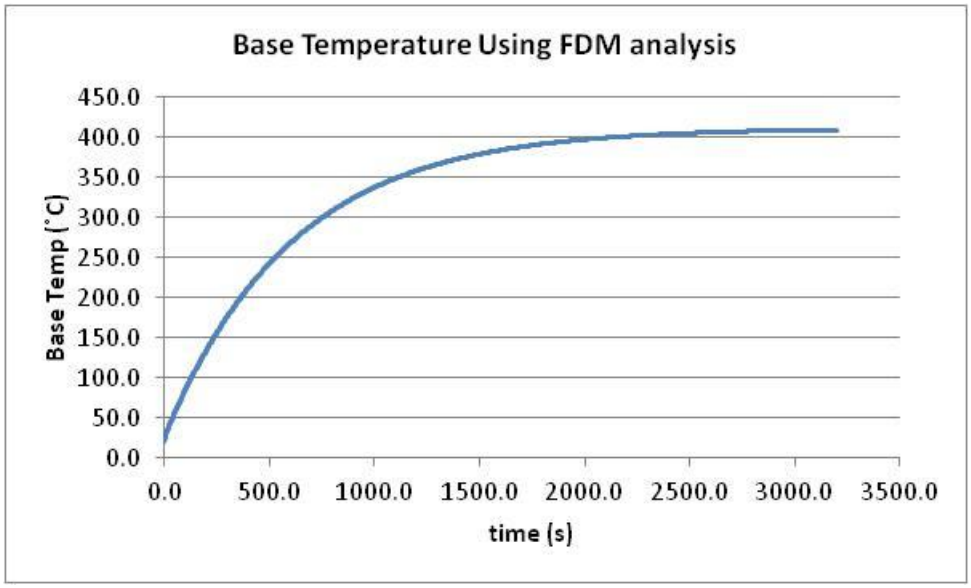

Fig. 16 Temperature of carabiner at contact point using FDM analysis

For a comparison of the FDM analysis to the lump capacitance and simplified fin analysis, see Fig 17 and Fig 18 .

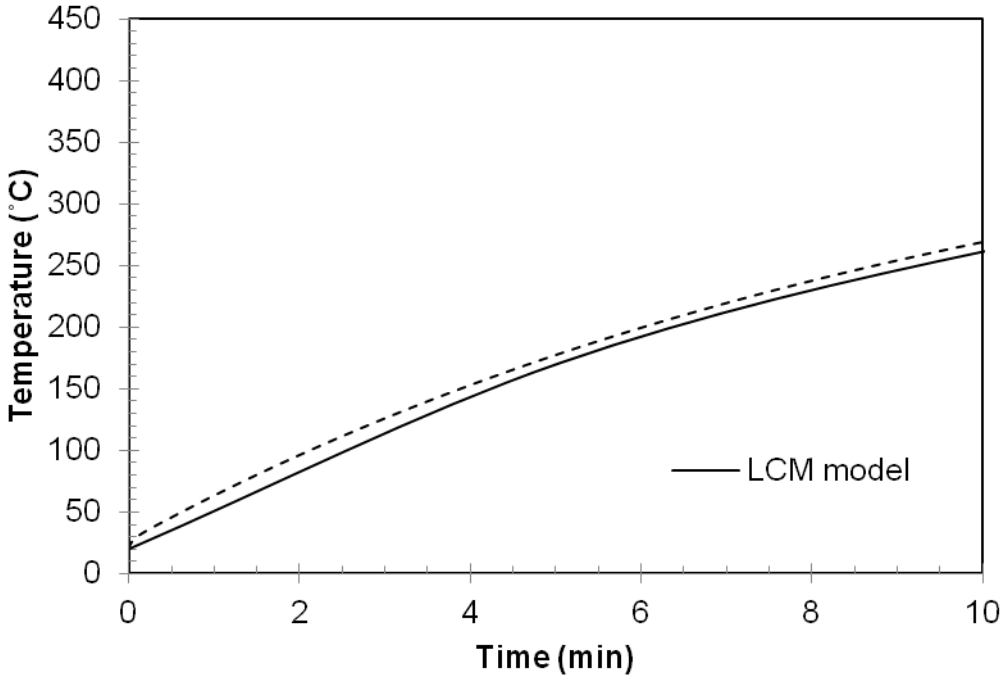

Fig. 17 Temperature versus time for lumped capacitence model (LCM) and from 1-D transient finite difference method at location of heat source. (Used with permission by Dr. Shollenberger).

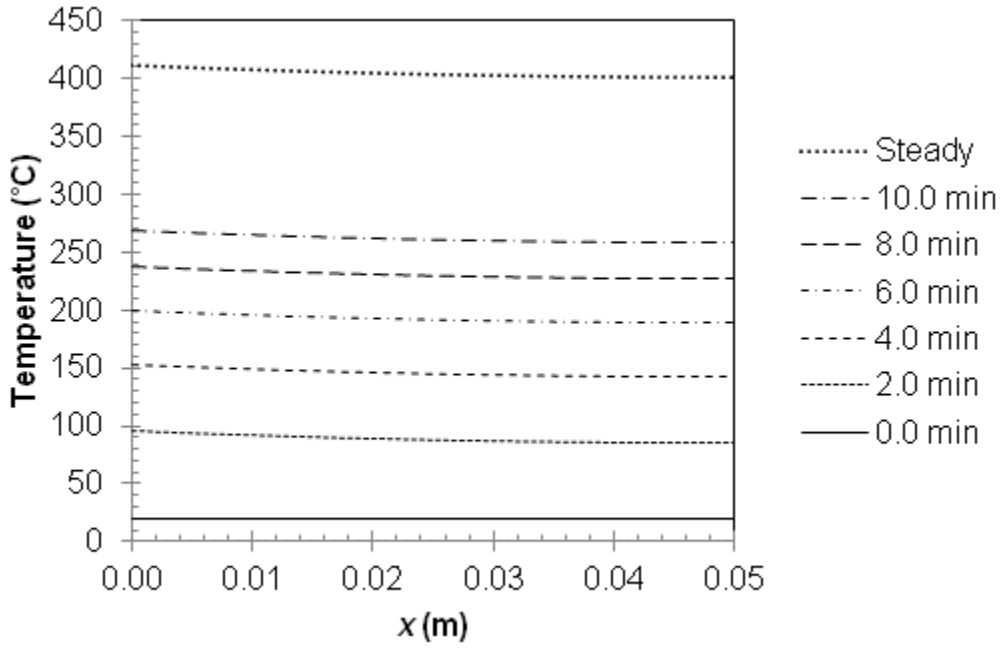

Fig. 18 Temperature versus location and time from finite difference method. Solution is converging to steady state fin solution as time increases. (Used with permission by Dr. Shollenberger).

The results of this analysis were interesting, because although the steady state temperature of the carabiner was approximately 337˚C, steady state should not be reached until about an hour after the heating begins and according to this model, it would take 9.8 minutes to reach the melting temperature

of 220˚C . The entire fatigue treatment only took approximately 14minutes to complete, and the carabiner was switched about every 1.4minutes, so according to this model, frictional heating alone would not result in melting of the rope fibers. What this analysis does not take into account is the increase in the dynamic friction coefficient between the rope and aluminum with the addition of dirt particles. When the frictional coefficient is doubled from .123 (that of clean rope) to .246, the steady state temperature rises to approx 801˚C and it only takes 2.8minutes to reach the melting temperature, see Fig 19.

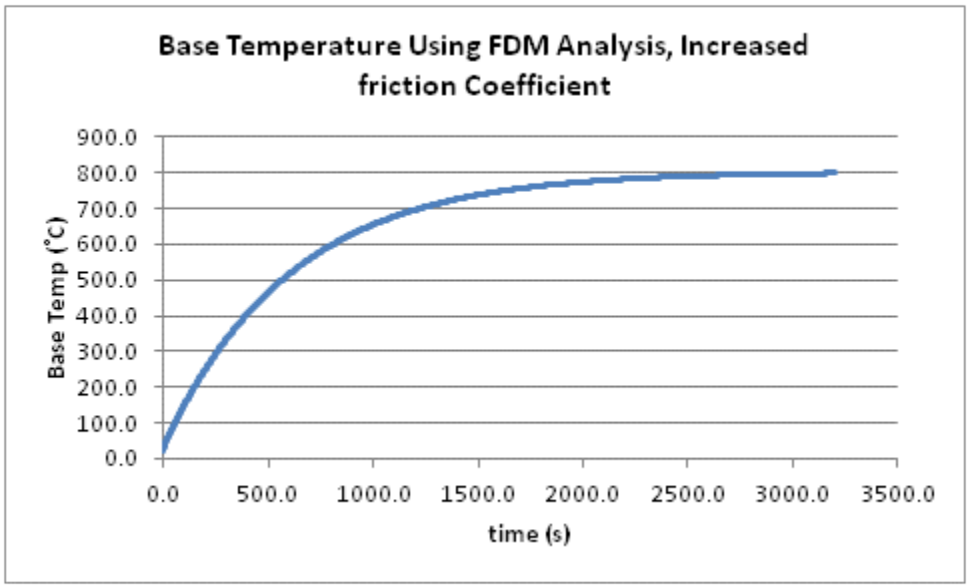

Fig. 19 FDM using increased friction coefficient due to addition of soil particles

This is concurrent with our results, as the untreated ropes showed no signs of melting, while the treated ropes exposed to 400 and 500 fatigue treatment cycles both exhibited some melting in the core fibers. Based on this analysis, and realizing that this is a conservative model, it is entirely plausible that frictional heating led to melting of the rope fibers.

The heat that builds up due to friction during a belay is not isolated to this controlled treatment, however. Frictional heat is always present. In operation, this heat is intensified by greater kinetic forces, various environments, more abrasive equipment and heavier loads exerted by 50 kg climbers falling from greater heights. Due to this thermal sensitivity, rope maintenance is critical. Fortunately proper rope cleaning is only needed occasionally. But a strictly adhered to washing routine to insure near maximum performance throughout the recommended lifetime of the rope should be observed.

Conclusion:

Based on the results of this project, it seems that abrasive particles found in soil will reduce the life of nylon fiber ropes. Although the testing methods were not perfect, it was clearly shown that under the testing conditions, rope exposed to a well graded soil prior to fatigue treatment experienced a much greater reduction in tensile strength than their untreated counterparts. It should be noted that the clean and dirty rope segments had identical strengths before fatigue treatment (5500lb break strength), the same as that of new rope (100% overall strength). Once exposed to fatigue treatment, the dirty ropes' overall strength dropped much more quickly than that of the untreated rope. After 500 fatigue cycles, the treated rope experienced a drop in strength of 79% as opposed to the untreated rope which only saw a 2% drop in strength. From this it has been determined that abrasive particles do decrease the fatigue life of nylon fiber ropes. The possible modes of this reduction are physical damage done to the core fibers by the soil particles, and melting or recrystalizing of the core fibers as a result of frictional heating, which did not occur in the untreated ropes. It is inferred that the increase in heating is a result of an increase in the dynamic friction coefficient between the nylon rope and aluminum carabiner due to the addition of soil particles.

Appendix A: Specific Vocabulary Definitions

Kernmantle: rope constructed with its interior core (the kern) protected with a woven exterior sheath (mantle) that is designed to optimize strength, durability, and flexibility.

Caprolactam: a polymerizing molecule that acts as a precursor to Nylon 6. Caprolactam is heated to 533K in a pure nitrogen atmosphere for 4-5 hours and pulled through spinnerets to form the nylon 6 fibers.

Diacid: Dicarboxylic acids are organic compounds that contain two carboxylic acid functional groups.

Diamine: A compound whose molecule contains two amino groups, esp. when not part of amide groups

Finite Difference Method (FDM): Finite-Difference methods are numerical methods for approximating the solutions to differential equations using difference equations to approximate derivatives. In this report, FDM analysis is used to model the temperature distribution with respect to time in an aluminum carabiner.

Appendix B: Specific Hand Calculations

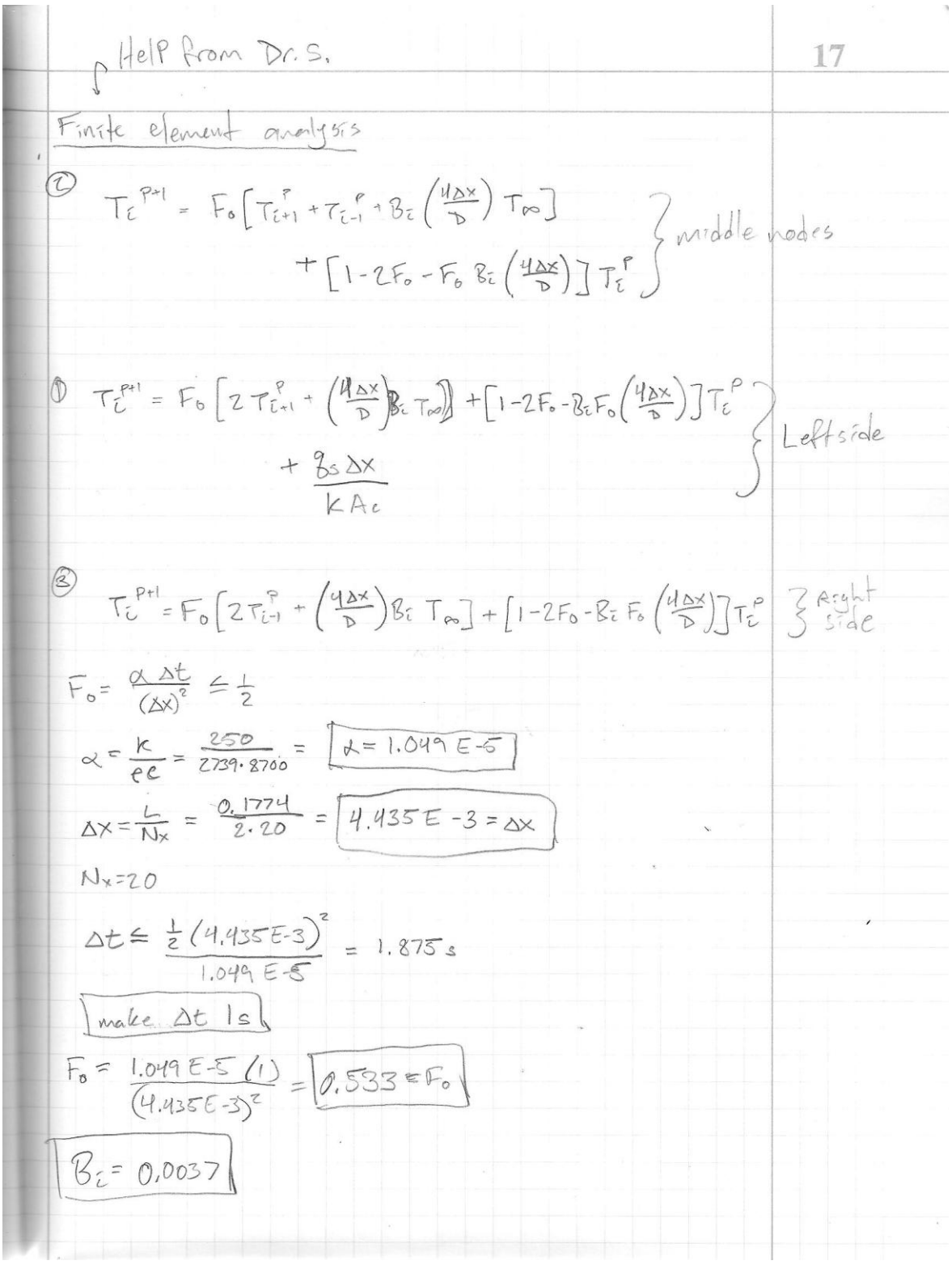

Help from Dr. S. 17

Finite element analysis

(2) $$T_i^{p+1} = F_o\left[T_{i+1}^p + T_{i-1}^p + B_i\left(\frac{4\Delta x}{D}\right)T_\infty\right] + \left[1 - 2F_o - F_o B_i\left(\frac{4\Delta x}{D}\right)\right]T_i^p$$ } middle nodes

(1) $$T_i^{p+1} = F_o\left[2T_{i+1}^p + \left(\frac{4\Delta x}{D}\right)B_i T_\infty\right] + \left[1 - 2F_o - B_i F_o\left(\frac{4\Delta x}{D}\right)\right]T_i^p + \frac{q_s \Delta x}{kA_c}$$ } Left side

(3) $$T_i^{p+1} = F_o\left[2T_{i-1}^p + \left(\frac{4\Delta x}{D}\right)B_i T_\infty\right] + \left[1 - 2F_o - B_i F_o\left(\frac{4\Delta x}{D}\right)\right]T_i^p$$ } Right side

$$F_o = \frac{\alpha \Delta t}{(\Delta x)^2} \leq \frac{1}{2}$$

$$\alpha = \frac{k}{\rho c} = \frac{250}{2739.8700} = \boxed{\alpha = 1.049\,E\text{-}5}$$

$$\Delta x = \frac{L}{N_x} = \frac{0.1774}{2.20} = \boxed{4.435\,E\text{-}3 = \Delta x}$$

$N_x = 20$

$$\Delta t \leq \frac{\frac{1}{2}(4.435E\text{-}3)^2}{1.049\,E\text{-}5} = 1.875\,s$$

make Δt 1s

$$F_o = \frac{1.049\,E\text{-}5\,(1)}{(4.435E\text{-}3)^2} = \boxed{0.533 = F_o}$$

$\boxed{B_i = 0.0037}$

What is steady state temp if modeled as Fin?

$h = 10$

$q_{in} = q_f = \eta_f \bar{h} A_f \theta_b$; $\theta_b = T_b - T_\infty$

$\eta_f = \frac{\tanh(mL)}{mL}$; $m = \left(\frac{4h}{kD}\right)^{1/2}$ | $A_f = \pi D \frac{L}{2}$

$= 0.00279$

$= \frac{\tanh(4(0.1774))}{4(0.1774)}$ $m = \sqrt{\frac{4(10)}{250(0.01)}}$

$m = 4$

$\eta_f = 0.86$

$T_b = \frac{q_{in}}{\eta_f \bar{h} A_f} + T_\infty$

$= \frac{29.24}{0.86(10)(0.00279)} + 298$

$\boxed{T_b = 1516.6\ K}$ for fin

~~how long does it take to reach steady state for temp capacitance?~~

273
+ 220
493

$T - T_\infty = b\tau\left[1 - \exp\left(-\frac{t}{\tau}\right)\right]$

$h = 10$

$b = \frac{Q}{\rho \forall C}$

$\tau = \frac{\rho \forall C}{h A_s}$

$\rho = 2739\ kg/m^3$

$C = 0.87\ kJ/kg\,K \cdot \frac{1000\ J}{1\ kJ} = 870\ J/kg\,K$

$D = 0.01m$

$k = 250\ W/m\,K$

$\forall = \frac{\pi}{4} D^2 L = 1.393E5$

$L = 0.1774m$

$T = 220°C = 493K$

$A_s = \pi D L = 0.005573$

$T_\infty = 25°C = 298K$

$Q = \frac{33.76 + 24.72}{2} = 29.24W$

$t = \ln\left(\frac{(T - T_\infty)}{b\tau} - 1\right)(-\tau)$

must Recalculate for new C

$t = \ln\left(1 - \frac{(T - T_\infty)}{b\tau}\right)(-\tau)$

$b = \frac{29.24}{2739 \cdot 1.393E-5 \cdot 870} = 0.8811$

$\tau = \frac{2739 \cdot 1.393E-5 \cdot 870}{10 \cdot 0.005573} = 595.63$

$t = (-\tau)\ln\left(\frac{(T - T_\infty)}{b\tau} - 1\right)$

$= (-595.63)\ln\left(1 - \frac{(493 - 298)}{0.881 \cdot 595.63}\right)$

$= (-595.63)(-0.1165)$

$t = 276.722\ s$

Time it will take to reach 220°C (T_m) assuming Constant Temp throughout carabiner.

calc B_i $\quad B_i = \frac{hD}{k}$ or $\frac{hL}{k} = \frac{10(0.1774)}{250} = 0.007$

$= \frac{10(0.01)}{250} = 4E-4$

B_i should be less than 0.1 ✓ $\quad Av B_i = 0.0057$

$$F_N = \sqrt{F_g^2 + \left(W_{TOT} + W_{TOT} - F_S\right)^2}$$

$$= \sqrt{59.65^2 + \left(205.46 \cdot 2 - 59.65\right)^2}$$

$$\boxed{F_N = 356.29\ N}$$

$$Q = \mu F_N V$$

$$= 0.123(356.29)(0.564)$$

$$\boxed{Q = 24.72\ W} \qquad \boxed{Q_{avg} = 29.24\ W}$$

$$q = \frac{Q}{A_c} = \frac{24.72}{1.57E{-}4}$$

for when bucket is pulling down →

$$\boxed{q = 1.575\ E5\ W/m^2}$$

H.T. Analysis (use larger q first)

$T_\infty = 25°C = 298K$

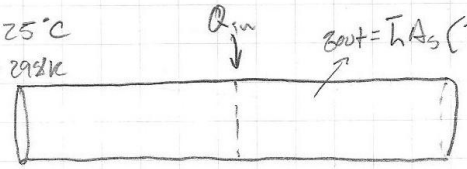

• assume uniform T in Aluminum
• assume Nat. convection with $\bar{h} = 5\text{-}10\ W/m^2K$

$\dot{E}_{in} - \dot{E}_{out} + \cancel{\dot{E}_g}^{\,0} = \cancel{\dot{E}_{st}}^{\,0}$: steady state

$q_{in} = q_{out} = \bar{h} A_s (T - T_\infty)$; $A_s = \pi D \cdot \frac{L}{2}$

$A_s = 0.002787\ m^2$

$D = 0.01\ m$

$L = 0.1774\ m$

solve for ~~$\bar{h}$~~ and $\bar{h} = 10$

$$T = \frac{q_{in}}{\bar{h} A_s} + T_\infty = \frac{33.76}{10 \frac{W}{m^2 K} \cdot 0.002787\ m^2} + 298K$$

$$\boxed{T_{steady} = 1509.33\ K}$$

need to calculate how long it takes to get to 220°C

Then, if possible, find time it would take for Nylon to heat to 220°C (melting point according to wikipedia

length of rope = 0.9144 m , length of heating area = $\frac{2\pi(0.005)}{2}$ = 0.01571 m

V = 0.564 m/s only interested in center of rope

assume whole length of rope is passed through carabiner and velocity is constant, treat as if going in circle

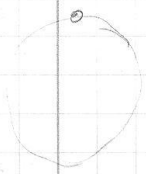

time to pass whole rope:

$\frac{L}{V} = \frac{0.9144}{0.564} = 1.621\,s$

time to pass 1 point

$\frac{L}{V} = \frac{0.01571}{0.564} = 0.02785\,s$

every 1.621 seconds, point of interest is exposed to heat for 0.02785 s

Now: calculate Q for when bucket weight is pulling Down:

FBD

assume T is in Y direction only

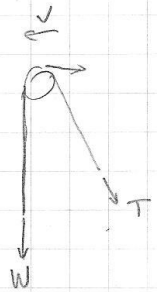

$T_2 = T_1 e^{\mu\beta}$

$T_2 = W_{TOT}$

$T_1 = W_{TOT} - F_f$

$\mu_k = 0.123$

$\beta = 2.793\,rad$

$W_{TOT} = 205.146\,N$

$W_{TOT} = e^{0.123(2.793)}(W_{TOT} - F_f)$

$F_f = -\left(\frac{W_{TOT}}{e^{0.123(2.793)} - W_{TOT}}\right) = 205.146 - \frac{205.146}{e^{0.123(2.793)}}$

$F_{f_{Bucket\ down}} = 59.65\,N$

Heat Transfer Model:

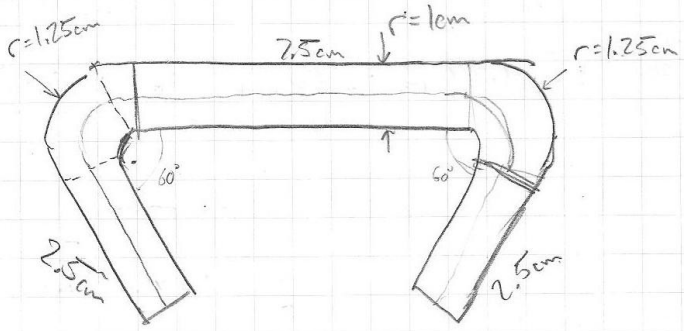

$C = 2\pi r$

$\frac{2\pi r}{180} = \frac{L}{60}$

$L = \frac{60 \cdot 2\pi r}{180} = 2.618\text{cm}$

$L_{TOT} = 2(2.5) + 7.5 + 2(2.618)$

$\boxed{L_{TOT} = 17.736\text{cm} = 0.1774\text{m}}$

model:

in open air, 25°C

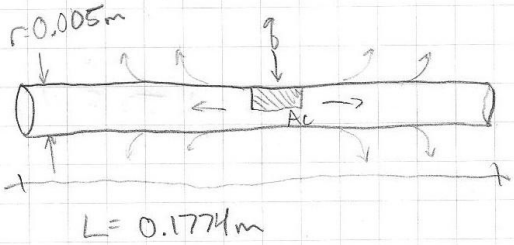

$A_c = 1.57E\text{-}4\ m^2$

$q = 2.15\ E\ 5\ W/m^2$

initial condition rope & aluminum start @ 25°C

Find: steady state temperature of aluminum

F_{sup} ① $= \sqrt{F_s^2 + (2W_{rot} + F_s)^2}$

F_{sup} ① $= 471.92N$ F_{sup} ② $= 501.47N$ → 6% variation, will use average

$F_{sup} = \boxed{F_N = 486.695N}$

Heating:

$F_s = \mu F_N$

$Q = \mu F_N V$; Q = ~~Heat~~ thermal energy generation
V = velocity

$q = \frac{Q}{A_c}$; q = heat flux
A_c = contact area

$Q = 0.123(486.695)(0.564) = 33.76 \frac{N \cdot m}{s} W$

$\boxed{Q = 33.76 W}$ $Q_{av.} =$

Model A_c:

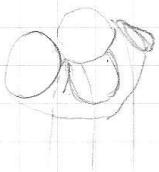

$A_c = \frac{2\pi r \cdot L}{2} = \frac{2\pi(0.005)(0.01)}{2}$

$\boxed{A_c = 1.57 E\text{-}4 m^2}$; $\boxed{q = 2.15 E5 W/m^2}$

Thermal conductivity k: (@25°c)

Nylon: 0.26 W/m·K

Aluminum: 250 W/mK

$\frac{g}{cm^3} \cdot \frac{1kg}{1000g} \cdot \frac{100^3 cm^3}{m^3} =$

Density: ρ
Nylon: 1090 kg/m³
Aluminum: 2739 kg/m³

specific heat C_p:
Nylon: 1.5 J/gK
Aluminum: 0.87 kJ/kgK = 870 J/kgK

$\Sigma F_x = F_{supx} - F_f = 0$ → $F_f = F_{supx}$

$\Sigma F_y = F_{supy} - W_{TOT} - T = 0$

$T = W_{TOT} + F_f$

$F_f = \mu_k |F_{sup}|$

$F_{sup} = \sqrt{F_{supx}^2 + F_{supy}^2}$

$\mu_k = 0.123$

$W_{TOT} = 205.146N$

7 eq

$F_{supx}, F_f, F_{supy}, W_{TOT}, T, \mu_k, F_{sup}$

$F_{supy} - W_{TOT} - W_{TOT} - F_f = 0$

$F_{supy} = 2W_{TOT} + F_f$

$F_{sup} = \sqrt{F_f^2 + F_{supy}^2} = \sqrt{F_f^2 + (2W_{TOT} + F_f)^2}$

$F_f = \mu_k \sqrt{F_f^2 + (2W_{TOT} + F_f)^2}$

$T = W_{TOT} + \mu_k \sqrt{F_{supx}^2 + F_{supy}^2}$

$F_{supy} - W_{TOT} - W_{TOT} - \mu_k \sqrt{F_{supx}^2 + F_{supy}^2} = 0$

$F_{supx} = \mu_k \sqrt{F_{supx}^2 + F_{supy}^2}$

beside:

$T_2 = T_1 e^{\mu\beta}$

$T_2 = T$

$T_1 = W_{TOT}$

$\mu = 0.123$

$\beta = 2.793$ rad

$T = W_{TOT} e^{\mu\beta}$

$T = W_{TOT} e^{\mu\beta} \rightarrow T = 289.24$

$\mu_k \sqrt{F_{supx}^2 + F_{supy}^2} = F_{supx}$

$0 = F_f - \mu_k \sqrt{F_f^2 + (2W_{TOT} + F_f)^2}$

$0 = F_f - 0.123 \sqrt{F_f^2 + (2 \cdot 205.146 + F_f)^2}$

① $F_f = 58.046N$ just using FBD eqns

using FBD + capstan eq.

$F_f = T - W_{TOT}$

$= W_{TOT} e^{\mu\beta} - W_{TOT}$

$= 205.146 \left(e^{.123(2.793)} - 1 \right)$

② $F_f = 84.095N$

FBD (carabiner)

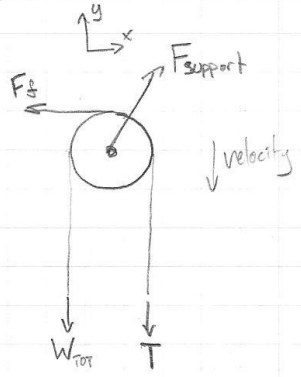

$\Sigma F_x = F_{support\,x} - F_f = 0$

$\Sigma F_y = F_{support\,y} - W_{TOT} - T = 0$

$T = W_{TOT} + F_f$

$F_f = \mu_k |F_{support}|$

finding μ_k:

average $\frac{\mu_s}{\mu_k} = 2.037$

μ_s (Nylon/Aluminum) = 0.25

μ_k (Nylon/Aluminum) = $\frac{\mu_s}{2.037} = \frac{0.25}{2.037} = 0.123$

$\boxed{\mu_k = 0.123}$

$T_1 = W$

$T_2 = 205.146\, e^{0.123(2.793)}$

$\boxed{T_2 = 289.24 N}$

does μ_k depend on units?

$F_f = \mu_s F_N$

$\mu_s = \frac{F_f}{F_N}$ ⇝ unitless, so no.

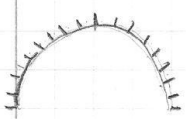

capstan equation (for rope ~~bering~~ friction over a drum

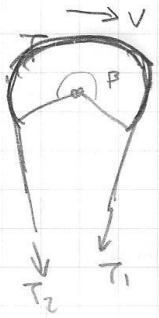

$T_2 = T_1 e^{\mu\beta}$

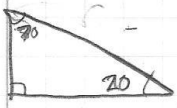

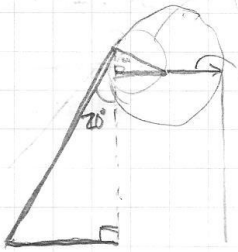

$\beta = 180 - 20 = 160° * \frac{\pi}{180} =$

$\boxed{\beta = 2.793 \text{ rad}}$

CALCULATIONS FOR DETERMINING FRICTIONAL HEAT TRANSFER TO ROPE.

FRICTION FORCE:

FBD (sys + cm)

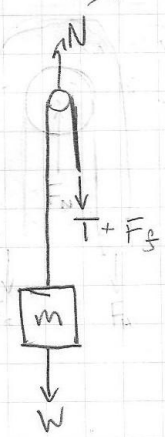

MAD

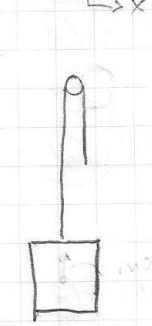

assume massless rope + carabiner
assume no acceleration
assume carabiner is rigid support

(this is for middle of cycle, not at top or bottom

find weight $W = mg$; $m = \rho V$; $\rho = 110 lb/ft^3$ $V = 3 gal$

$W_{sand} = \frac{110 lb}{ft^3} \cdot 3 gal \cdot \frac{0.1337 ft^3}{1 gal} \cdot \frac{4.448 N}{lb} = 196.25 N$

find velocity ↓ + W_{bucket} (216 = 8.896N) (44.1216) seems right

$W_{TOT} = 205.146 N$

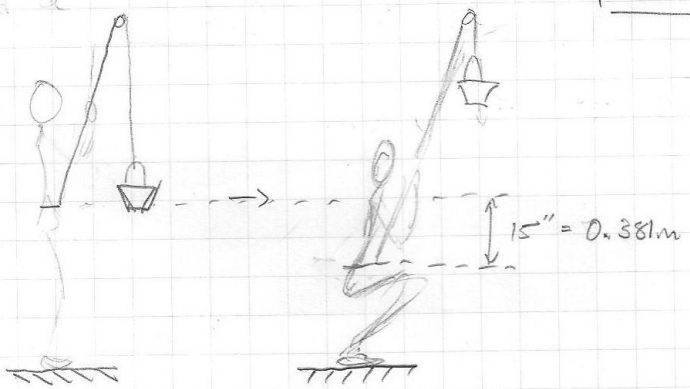

20 up downs = 27 seconds

$\frac{20 \text{ updown}}{27 s} \times \frac{2 \cdot 0.381 m}{1 \text{ updown}} = 0.564 m/s$

$V = 0.564 m/s$

References:

[1] Alberts, Alfred W. "Educational Content Archive." *CHF Legacy Content*. 17 Oct. 2011. Web. 03 Feb. 2012. <http://assets.chemheritage.org/>.

[2] Attaway, Stephen W. *The Mechanics of Friction in Rope Rescue*. Tech. International Technical Rescue Symposium. Print.

[3] "Benzene." *Benzene*. ECO-USA. Web. 03 June 2012. <http://www.eco-usa.net/toxics/chemicals/benzene.shtml>.

[4] Beyerlein, Adolph. *Http://nylene.com/nylene_pdfs/clemson_university_report.pdf*. Rep. Clemson University. Web.

[5] "Cyclohexane." *3DChem.com*. Web. 03 June 2012. <http://www.lindane.org/chemicals/cyclohexane.htm>.

[6] Flory, John F., and David E. Mercer. *The New Cordage Institute Fiber Rope Test Methods*. 0-7803-4108-2. Morristown: Tension Technology International. Print.

[7] "Goes Around, Comes." *Goes Around, Comes*. Web. 03 June 2012. <http://materialconnexion.com/Home/Matter/MatterMagazine81/PastIssues/MATTER44/GoesAroundComes/tabid/203/Default.aspx>.

[8] Huntley, Mark B., and A. Simeon Whitehill. *Retirement Criteria for Nylon Ropes*. Working paper no. 0-7803-7534-3. Chester: Whitehill Manufacturing Corporation, 2002. Print.

[9] MacKetta, John J. *Encyclopedia of Chemical Processing and Design*. New York U.a.: Dekker, 1978. Print.

[10] "Nexis Fibers." *System & Conversion Yarn Description : Yarn Description*. Web. 03 June 2012. <http://www.nexisfibers.com/spip.php?rubrique76>.

[11] Nichols, Jeff, Stephen Banfield, and John Flory. *Forensic Techniques for Investigating the Causes of Fiber Rope Failures*. Tech. Arbroath: Tension Technology International. Print.

[12] Sloan, F., S. Bull, and R. Longerich. *Design Modifications to Increase Fatigue Life of Fiber Ropes*. Tech. Cortland: Cortland Companies. Print.

[13] United States. Environmental Protection Agency. *Modifications To The 112(b)1 Hazardous Air Pollutants*. Print.

[14] Woll, Tim. "Cyclohexane." *Cyclohexane*. Chevron Phillips. Web. 03 June 2012. <http://www.cpchem.com/bl/aromatics/en-us/Pages/Cyclohexane.aspx>.